Published in final edited form as:
J Am Chem Soc. 2010 January 20; 132(2): 647–655. doi:10.1021/ja907523x.

On the Chalcogenophilicity of Mercury: Evidence for a Strong Hg–Se Bond in [Tm$^{Bu^t}$]HgSePh and its Relevance to the Toxicity of Mercury

Jonathan G. Melnick, **Kevin Yurkerwich**, and **Gerard Parkin**
Department of Chemistry, Columbia University, New York, New York 10027, USA

Jonathan G. Melnick: ; Kevin Yurkerwich: ; Gerard Parkin: parkin@columbia.edu

Abstract

One of the reasons for the toxic effects of mercury has been attributed to its influence on the biochemical roles of selenium. For this reason, it is important to understand details pertaining to the nature of Hg–Se interactions and this has been achieved by comparison of a series of mercury chalcogenolate complexes that are supported by *tris*(2-mercapto-1-t-butyl-imidazolyl)hydroborato ligation, namely [Tm$^{Bu^t}$]HgEPh (E = S, Se, Te). In particular, X–ray diffraction studies on [Tm$^{Bu^t}$]HgEPh demonstrate that although the Hg–S bonds involving the [Tm$^{Bu^t}$] ligand are *longer* than the corresponding Cd–S bonds of [Tm$^{Bu^t}$]CdEPh, the Hg–EPh bonds are actually *shorter* than the corresponding Cd–EPh bonds, an observation which indicates that the apparent covalent radii of the metals in these compounds are dependent on the nature of the bonds. Furthermore, the difference in Hg–EPh and Cd–EPh bond lengths is a function of the chalcogen and increases in the sequence S (0.010 Å) < Se (0.035 Å) < Te (0.057 Å). This trend indicates that the chalcogenophilicity of mercury increases in the sequence S < Se < Te. Thus, while mercury is often described as being thiophilic, it is evident that it actually has a greater selenophilicity, a notion that is supported by the observation of facile selenolate transfer from zinc to mercury upon treatment of [Tm$^{Bu^t}$]HgSCH$_2$C(O)N(H)Ph with [Tm$^{Bu^t}$]ZnSePh. The significant selenophilicity of mercury is in accord with the aforementioned proposal that one reason for the toxicity of mercury is associated with it reducing the bioavailability of selenium.

Introduction

The potent toxicity of mercury compounds is often associated with the high affinity of mercury for sulfur, such that it binds effectively to the cysteine residues in proteins and enzymes, thereby perturbing their functions.[1,2,3] Another mechanism for the toxicity of mercury, however, has been attributed to its impact on the biochemical roles of selenium,[4] an essential trace element.[5] Indeed, as a constituent of selenoproteins derived from selenocysteine and selenomethionine,[6] selenium has been described as the most important antioxidant element in the human body and selenium deficiency has been linked to cancer and neurodegenerative diseases.[4] On this basis, the toxicity of mercury has also been attributed to *(i)* the interaction between between Hg(II) and selenium compounds reducing the bioavailability of selenium *via* the formation of insoluble mercury selenide species[7] and *(ii)* mercury binding to the active sites of selenoenzymes, thereby inhibiting their functions.[8] Furthermore, while high concentrations of selenium are toxic,[4,5] addition of selenite (Na_2SeO_3) has actually been observed to have a detoxifying effect on mercury.[7,9] It is, therefore, evident that the toxic effects of mercury and

Correspondence to: Gerard Parkin, parkin@columbia.edu.

selenium are strongly intertwined and, for this reason, it is important to establish details concerned with the nature of Hg–Se interactions. Herein, we report a series of studies to address this issue by assessing the structures of mercury chalcogenolate complexes and the thermodynamics associated with the binding of such ligands to mercury.

Results and Discussion

We have recently utilized the *tris*(2-mercapto-1-R–imidazolyl)hydroborato ligand system, [Tm^R], to provide a platform for mimicking the coordination of metals, such as zinc and mercury, to cysteine rich sites of proteins.[10,11,12] As an extension of these investigations, we sought to establish the extent to which selenium ligands bind mercury in preference to its congener zinc, a comparison that is particularly appropriate in view of the fact that zinc is essential for human life whereas mercury is highly toxic. To achieve this objective, we compare here the structures of a series of chalcogenolate complexes [Tm^{Bu^t}]MEPh (M = Zn, Cd, Hg; E = S, Se, Te) and assess the preference for phenylselenolate to coordinate to mercury rather than to zinc.

1. Syntheses and Structures of a Series of Mercury Phenylchalcogenolate Complexes

Our recent studies concerned with a functional model of mercury detoxification by the organomercurial lyase, *MerB*, have demonstrated that the phenylthiolate complex [Tm^{Bu^t}]HgSPh may be obtained *via* the reactions of the mercury alkyl compounds [κ^1– Tm^{Bu^t}]HgR (R = Me, Et) with PhSH.[10] Extending this result, the phenylselenolate counterpart [Tm^{Bu^t}]HgSePh may likewise be obtained *via* treatment of [κ^1–Tm^{Bu^t}]HgEt with PhSeH, while the phenyltellurolate complex [Tm^{Bu^t}]HgTePh may be synthesized *via* the reaction of [κ^1–Tm^{Bu^t}]HgEt with Ph_2Te_2 (Scheme 1). The molecular structures of [Tm^{Bu^t}]HgEPh (E = S,[13] Se, Te) have been determined by X–ray diffraction, as illustrated in Figures 1 – 3, and the Hg–E bond lengths (Table 1) are comparable to the respective values in $[Hg(EPh)_3]^-$ (E = S,[14] Se,[15] Te[16]).

Since the molecular structures of [Tm^{Bu^t}]HgSPh, [Tm^{Bu^t}]HgSePh and [Tm^{Bu^t}]HgTePh complete the first series of structurally characterized phenylchalcogenolate complexes of zinc, cadmium and mercury, namely [Tm^{Bu^t}]MEPh (M = Zn,[17] Cd,[18] Hg; E = S, Se, Te), it is pertinent to evaluate the structural details associated with the M–EPh bond, as summarized in Table 1. Firstly, however, it is important to note that the metal centers of all of the complexes have a common *pseudo*-tetrahedral coordination geometry, with the [Tm^{Bu^t}] ligand binding in a κ^3–mode with similar bond lengths, as judged by the small standard deviations for the average values (Table 1). For example, for the phenyltellurolate complexes, the Zn–S bond lengths in [Tm^{Bu^t}]ZnTePh range from 2.35 – 2.37 Å, while the Hg–S bond lengths in [Tm^{Bu^t}]HgTePh range from 2.58 – 2.64 Å. Also noteworthy, the average M–S bond length for [Tm^{Bu^t}]MEPh complexes is effectively independent of the nature of the chalcogenolate ligand (Table 1 and Figure 4). For example, the average Hg–[Tm^{Bu^t}] bond lengths for [Tm^{Bu^t}]HgEPh range from 2.59 Å for [Tm^{Bu^t}]HgSPh to 2.60 Å for [Tm^{Bu^t}]HgTePh. Furthermore, for a given chalcogen, the M–[Tm^{Bu^t}] bond lengths progressively increase in the sequence Zn < Cd < Hg (Figure 4).

In contrast to the monotonic variation in M–[Tm^{Bu^t}] bond lengths, the M–EPh bond lengths increase in the irregular sequence Zn < Hg < Cd, with the cadmium derivative having the longest bond in each case (Table 1 and Figure 5). Thus, the phenylchalcogenolate complexes, [Tm^{Bu^t}]MEPh, represent an interesting series of compounds that exhibit *two different trends* in M–X bond length as a function of the metal.

Examination of the literature indicates that while Hg–X and Cd–X bond lengths in structurally related covalent compounds are comparable (Table 2), Hg–X bonds are, in many cases, distinctly shorter than the corresponding Cd–X bonds. This trend is in accord with the covalent

radius of mercury (1.32 Å) being smaller than that of cadmium (1.44 Å),[19] an observation that may be rationalized by a combination of the lanthanide contraction and relativistic effects.[20, 21,22,23] A simple illustration of the smaller size of mercury relative to cadmium is provided by Power's report that the M–M bonds in the dinuclear complexes ArM–MAr [M = Zn, Cd, Hg; Ar = C_6H_3-2,6-(C_6H_3-2,6-Pr^i_2)$_2$] vary in such a manner that the Cd–Cd bond is the longest: Zn–Zn = 2.3591(9) Å, Cd–Cd = 2.6257(5) Å, and Hg–Hg = 2.5738(3) Å.[24] Likewise, the M–CH_3 bonds in $M(CH_3)_2$[20] and the M–Sn bonds in [$MeSi\{SiMe_2N(p\text{-}Tol)\}_3Sn]_2M$[25] follow the same sequence, with the Cd–X bond being the longest in each case. In addition to these examples involving two-coordinate metal centers, the M–halogen bonds in tetrahedral [Tp^{Pri2}]MCl,[26] [Tm^R]MBr (R = Me, Bu^t),[27,28] and [Tse^{Mes}]MI,[29] exhibit the same trend, with the Cd–X (X = Cl, Br, I) bond being longer than the corresponding Hg–X bond in each case.

However, although Cd–X bonds are often longer than the corresponding Hg–X bonds, it is important to emphasize that this trend is not always followed. For example, analysis of the average bond length data listed in the Cambridge Structural Database[30] for a series of cadmium and mercury halide derivatives, $[MX_4]^{2-}$ (M = Cd, Hg; X = Cl, Br, I), indicates that the Cd–X bonds are actually *shorter* than the corresponding Hg–X bonds, as illustrated in Table 2. The same trend in M–X bond lengths is also observed for $(Ph_3P)_2MX_2$ (M = Cd, X = Cl,[31] I[32]; M = Hg, X = Cl,[33] I[34]) such that the Cd–X bonds are shorter than the Hg–X bonds; the corresponding M–P bonds, however, exhibit the opposite trend, with the Hg–P bonds being shorter than the Cd–P bonds (Table 2). It is, therefore, evident that the bond length changes observed for the cadmium and mercury compounds [Tm^{Bu^t}]MEPh and $(Ph_3P)_2MX_2$ illustrate interesting subtleties concerned with the notion of the "covalent radius" of an atom: *viz* the apparent covalent radius of the metal in these complexes is not only molecule dependent, but is also dependent on the nature of the bond.[35]

2. Structural Evidence for the Enhanced Selenophilicity and Tellurophilicity of Mercury

While the observation that the Hg–EPh bonds are shorter than the respective Cd–EPh bonds is in accord with the relative covalent radii of mercury and cadmium,[19] an important finding is that the difference in bond lengths is a function of the chalcogen. Specifically, the difference in Hg–EPh and Cd–EPh bond lengths increases in the sequence S (0.010 Å) < Se (0.035 Å) < Te (0.057 Å), such that the Hg–TePh bond becomes substantially shorter than the Cd–TePh bond (Figure 5).[36] Correspondingly, the difference in Hg–EPh and Zn–EPh bond lengths decreases in the sequence S (0.177 Å) > Se (0.130 Å) > Te (0.085 Å), again indicating that the Hg–TePh bond is unusually short.[36] It is, therefore, evident that Zn–EPh, Cd–EPh and Hg–EPh bond lengths do not scale equally with the covalent radii of the chalcogens.

A convenient means to portray the extent to which a specific M–EPh bond length deviates from an expected value is provided by normalizing the M–EPh (E = Se, Te) bonds relative to that for M–SPh and comparing the change in bond lengths relative to the change in covalent radius of the chalcogen (Figure 6). In this regard, examination of the data for the Zn, Cd, and Hg compounds [Tm^{Bu^t}]MEPh indicates that *all* M–SePh and M–TePh bond lengths are shorter than would be predicted on the basis of the value for the M–SPh bond length and the change in covalent radius of the chalcogen (Figure 6).[37,38] Furthermore, while the deviation is small for zinc, it is substantial for mercury. For example, the deviation of the M–TePh bond lengths from the predicted values increases considerably in the sequence Zn (0.034 Å) < Cd (0.080 Å) < Hg (0.126 Å). The deviation for mercury becomes even more significant when it is recognized that the variation in M–E (E = S, Se, Te) bond lengths for other metals correspond closely to the values predicted by the covalent radii of the chalcogens. For example, the maximum deviation in M–Te bond length for compounds of a variety of other metals is only 0.026 Å: Zr (–0.018 Å),[39] La (–0.002 Å),[40] Sm (0.004 Å),[41] U (0.020 Å),[40] Pu (0.026 Å).[40]

The structural data, therefore, reveal that mercury is exceptional with respect to its interactions with selenium and tellurium in the complexes described here. Mercury is well known to be thiophilic, having a high affinity for sulfur in its various forms; indeed, the propensity of mercury for sulfur is the origin of the term “mercaptan”, an abbreviated form of “mercurium captans”, which is Latin for “seizing mercury”. However, on the basis of the observed relative shortening of the Hg–Se and Hg–Te bond lengths, it is now evident that the selenophilicity and tellurophilicity of mercury actually surpass its thiophilicity,[42] an observation that is of considerable relevance for one of the proposed mechanisms of mercury toxicity, namely Hg (II) reducing the bioavailability of selenium.[7,8]

3. Relative Strengths of Hg–ER and Zn–ER Interactions

To complement the above structural studies, we sought to obtain thermodynamic data pertaining to the binding of the phenylselenolate ligand to mercury. In this context, while the equilibrium constant for the exchange reaction involving [Tm^{Bu^t}]HgSPh[10] and [Tm^{Bu^t}]ZnSePh[17] (Scheme 2, equation 1) would provide a direct indication of the relative tendency for mercury to bind the phenylselenolate ligand, measurement of the equilibrium constant by using ^{1}H NMR spectroscopy is complicated by the fact that the chemical shifts of the species involved in the equilibrium are not sufficiently distinct. Therefore, to facilitate the analysis, we decided to employ thiolate and selenolate ligands that bear different substituents. In particular, we decided to employ the recently reported zinc thiolate complex [Tm^{Bu^t}]$ZnSCH_2C(O)N(H)Ph$,[43] derived from *N*-phenyl-2-mercaptoacetamide $PhN(H)C(O)CH_2SH$, on the premise that the use of this substituent would enable measurement of the equilibrium constant for the thiolate/selenolate exchange reaction with [Tm^{Bu^t}]HgSePh (Scheme 2, equation 2). At the outset, therefore, an independent synthesis of the mercury thiolate component of the equilibrium mixture, [Tm^{Bu^t}]$HgSCH_2C(O)N(H)Ph$, was required.

The mercury thiolate [Tm^{Bu^t}]$HgSCH_2C(O)N(H)Ph$ complex may be synthesized *via* either reaction of *(i)* [κ^1–Tm^{Bu^t}]HgEt with $PhN(H)C(O)CH_2SH$ or *(ii)* [Tm^{Bu^t}]HgX (X = Cl, Br) with $PhN(H)C(O)CH_2SM$ (M = Li, K), as illustrated in Scheme 3. The molecular structure of [Tm^{Bu^t}]$HgSCH_2C(O)N(H)Ph$ has been determined by X–ray diffraction (Figure 7), thereby demonstrating that there is an intramolecular N–H•••S hydrogen bond between the amide N–H group and thiolate sulfur atom. This hydrogen bonding feature is also present in the zinc complex [Tm^{Bu^t}]$ZnSCH_2C(O)N(H)Ph$, but a notable aspect is that the interaction in the mercury complex is not as pronounced as that in the zinc complex. For example, the NH•••S and N•••S distances of 2.53(5) and 3.072(4) Å for [Tm^{Bu^t}]$HgSCH_2C(O)N(H)Ph$ are, respectively, both longer than the corresponding values of 2.42(4) Å and 3.004(4) Å for the zinc complex [Tm^{Bu^t}]$ZnSCH_2C(O)N(H)Ph$.[43] The greater hydrogen bonding interaction within the zinc complex [Tm^{Bu^t}]$ZnSCH_2C(O)N(H)Ph$ may be attributed to there being a greater ionic component to the Zn–S bond than the Hg–S bond, in accord with zinc being more electropositive than mercury.[44] The observation that the hydrogen bonding interaction is greater for the zinc compound [Tm^{Bu^t}]$ZnSCH_2C(O)N(H)Ph$ is also interesting because although the same trend has been observed for zinc and mercury pyrrol-2-ylmethyleneaminoethylthiolate complexes that feature NH•••S hydrogen bonds,[45] the opposite trend has been reported for 1,2-benzenedithiolate complexes.[46]

Treatment of the mercury thiolate [Tm^{Bu^t}]$HgSCH_2C(O)N(H)Ph$ with the zinc selenolate [Tm^{Bu^t}]ZnSePh results in the formation of the mercury selenolate complex [Tm^{Bu^t}]HgSePh and zinc thiolate [Tm^{Bu^t}]$ZnSCH_2C(O)N(H)Ph$ (Scheme 2, equation 2). Significantly, the reaction proceeds to completion, as indicated by the fact that treatment of [Tm^{Bu^t}]HgSePh with [Tm^{Bu^t}]$HgSCH_2C(O)N(H)Ph$ does not produce measurable quantities of [Tm^{Bu^t}]ZnSePh and [Tm^{Bu^t}]$HgSCH_2C(O)N(H)Ph$ by ^{1}H NMR spectroscopy. A lower limit for the equilibrium

constant for selenolate transfer to mercury (Scheme 2, equation 2) is estimated to be > 150 (see Experimental Section).

While this observation is in accord with the notion that mercury has a strong preference to bind the selenolate ligand, it is essential to consider the effect of the different substituents on the chalcogen, *i.e.* EPh *vs.* $ECH_2C(O)N(H)Ph$, in determining the overall thermodynamics. To address this issue, the equilibrium for the all–thiolate system, involving the reaction of $[Tm^{Bu^t}]HgSCH_2C(O)N(H)Ph$ with $[Tm^{Bu^t}]ZnSPh$ (Scheme 2, equation 3) was investigated. Importantly, the equilibrium constant is only 1.3(4), thereby indicating that the nature of the chalcogen substituents play little role in determining the thermodynamics of selenolate and thiolate ligand transfer between zinc and mercury (Scheme 2, equation 3).

The greater preference for mercury, relative to zinc, to bind to selenolate rather than thiolate in this system may be attributed to the sum of the Hg–Se and Zn–S bond energies being greater than the sum of the Hg–S and Zn–Se bond energies. An alternative and equivalent description is that the observed thermodynamics is a consequence of the difference in Zn–S and Zn–Se bond energies being greater than the difference in Hg–S and Hg–Se bond energies, *i.e.* $[D(Zn–S) – D(Zn–Se)] > [D(Hg–S) – D(Hg–Se)]$.

DFT calculations are in accord with the experimental observation and indicate that ΔH^{SCF} for the reaction between $[Tm^{Bu^t}]HgSCH_2C(O)N(H)Ph$ and $[Tm^{Bu^t}]ZnSePh$ (Scheme 2, equation 2) is exothermic by 4.54 kcal mol^{-1}. Further insight into the origin of the thermodynamics of the exchange reaction is provided by consideration of the individual heterolytic M–ER bond enthalpies (Table 3) that are not otherwise available experimentally. In accord with the exothermicity of the reaction between $[Tm^{Bu^t}]HgSCH_2C(O)N(H)Ph$ and $[Tm^{Bu^t}]ZnSePh$, the sum of the $Zn–SCH_2C(O)N(H)Ph$ and Hg–SePh bond enthalpies (212.58 kcal mol^{-1}) is greater than the sum of Zn–SePh and $Hg–SCH_2C(O)N(H)Ph$ bond enthalpies (208.04 kcal mol^{-1}). Furthermore, evaluation of the bond enthalpies demonstrates that the driving force for the exchange reaction is largely determined by the strength of the Hg–SePh bond (Table 3). Thus, while the Hg–SePh bond enthalpy is 6.06 kcal mol^{-1} greater than the $Hg– SCH_2C(O)N(H)Ph$ bond enthalpy, the corresponding Zn–SePh bond enthalpy is only 1.52 kcal mol^{-1} greater than the $Zn–SCH_2C(O)N(H)Ph$ bond enthalpy. As such, there is a strong driving force for the SePh ligand to transfer from zinc to mercury.

It is also instructive to compare the M–SeR and M–SR bond enthalpies for situations in which the chalcogens bear the *same* substituent. In this regard, comparison of the data in Table 3 indicates that the Hg–SePh bond is slightly stronger than the Hg– SPh bond, whereas the Zn–SePh bond is slightly weaker than the Zn–SPh bond. Consideration of the literature indicates that for many systems involving bonds to sulfur and selenium, *e.g.* E–H,[6d] E–C[6d], E–P,[47] and E–transition metal[48,49,50] (E = S, Se), the bond to sulfur is *generally* the stronger; however, there are situations in which the reverse is observed. For example, the opposite trend has been observed for coordination of thio- and selenoethers to transition metals.[51] It is, therefore, evident that there are subtleties concerned with relative M–S and M–Se bond energies.

In this regard, although there are very few studies that directly address the difference in Hg–S and Hg–Se bond energies, the formation constants for several MeHgSeR complexes from $[MeHg]^+$ are greater than the corresponding values for MeHgSR.[52,53] In addition, there is circumstantial evidence which suggests that Hg–Se interactions are stronger than corresponding Hg–S interactions. For example, $^2J_{Hg–H}$ for the methyl groups of the selenolate and selenourea complexes, MeHgSeR and $\{MeHg[SeC(NH_2)_2]\}^+$, are smaller than those for the corresponding thiolate and thiourea derivatives, CH_3HgSR and $\{[(H_2N)_2CS]HgMe\}^+$. The smaller $^2J_{Hg–H}$ coupling constants for the selenium compounds has been taken to imply that the Hg–C interactions are weaker than in the sulfur derivatives and, on this basis, it was

postulated that the Hg– Se interactions are stronger than the corresponding Hg–S interactions.[54,55] Moreover, comparison of the Hg–S and Hg–Se bond lengths of $MeHgSCH_2CH(NH_3)CO_2$ (2.352 Å) and $MeHgSeCH_2CH(NH_3)CO_2$ (2.469 Å) indicates that the difference (0.12 Å) is marginally less than would be expected on the basis of covalent radii of sulfur and selenium (0.15 Å),[19] an observation that was also interpreted in terms of a Hg–Se interaction that is stronger than otherwise expected.[54a] In this regard, the difference in Hg–S and Hg–Se bond lengths of $[Tm^{Bu^t}]HgSPh$ and $[Tm^{Bu^t}]HgSePh$ (0.07 Å) is even smaller than that for $MeHgSCH_2CH(NH_3)CO_2$ and $MeHgSeCH_2CH(NH_3)CO_2$ (0.12 Å), thereby suggesting a relatively stronger Hg–Se interaction for $[Tm^{Bu^t}]HgSePh$.

The body of evidence (which includes equilibrium, structural, and computational studies), therefore, demonstrates that (relative to zinc) mercury exhibits a stronger preference to coordinate to selenium rather than to sulfur. Thus, while mercury is typically regarded to be thiophilic and bind strongly to mercapto groups, it is evident that mercury possesses a greater selenophilicity relative to other metals. The enhanced preference for mercury to bind selenium is, nevertheless, in accord with the empirical classifications of Hg^{2+} as a class (b)[56] acceptor and as a soft[57] Lewis acid.[58]

The selenophilicity of mercury is of potential relevance to the chelation therapy that is used in the treatment of heavy metal toxicity. An ideal chelating agent is one that binds strongly to the desired metal but does not interact with other biologically essential metals. Such selectivity, however, is difficult to achieve and the chelating agents of choice for mercury poisoning, namely sodium 2,3-dimercaptopropanesulfate (DMPS) and *meso*-2,3-dimercaptosuccinic acid (DMSA), also chelate the essential elements copper, chromium and zinc.[3,59,60] The observation that selenium shows an exceptional preference for coordinating to mercury over zinc suggests that ligands which feature selenium (and possibly tellurium) donors may prove to be effective in mercury chelation therapy, and thereby provides an approach for the design of new chelation agents.

Conclusions

In summary, X–ray diffraction studies on the series of complexes $[Tm^{Bu^t}]ZnEPh$ (M = Zn, Cd, Hg; E = S, Se, Te) demonstrate that although the Hg–S bonds involving the $[Tm^{Bu^t}]$ ligand are *longer* than the corresponding Cd–S bonds, the Hg–EPh bonds are *shorter* than the corresponding Cd–EPh bonds. As such, it emphasizes that the apparent covalent radius of the metal in these complexes is not only molecule dependent, but is also bond dependent. Furthermore, the difference in Hg–EPh and Cd–EPh bond lengths in these complexes is a function of the chalcogen and increases in the sequence S (0.010 Å) < Se (0.035 Å) < Te (0.057 Å), a trend which reflects the chalcogenophilicity of mercury increasing in the sequence S < Se < Te. Thus, while mercury is often described as being thiophilic, it is evident that it actually has a much greater selenophilicity, an observation that is of considerable relevance for one of the proposed mechanisms of mercury toxicity in which Hg(II) reduces the bioavailability of selenium.

Experimental Section

General Considerations

All manipulations were performed using a combination of glovebox, high-vacuum and Schlenk techniques under a nitrogen or argon atmosphere, except where otherwise stated. Solvents were purified and degassed by standard procedures. NMR spectra were measured on Bruker 300 DRX and Bruker 400 DRX spectrometers. For solutions in organic solvents, ^1H NMR spectra are reported in ppm relative to $SiMe_4$ ($\delta = 0$) and were referenced internally with respect to the protio solvent impurity (δ 7.16 for C_6D_5H,[61] δ 5.32 for $CHDCl_2$[62]). ^{13}C NMR spectra are

reported in ppm relative to $SiMe_4$ ($\delta = 0$) and were referenced internally with respect to the solvent (δ 128.06 for C_6D_6).[61] Coupling constants are given in hertz. IR spectra were recorded as KBr pellets on a Nicolet Avatar DTGS spectrometer, and the data are reported in reciprocal centimeters. Mass spectra were obtained on a JMS-HX110/110 Double Focusing mass spectrometer using fast atom bombardment (FAB). Combustion analyses were carried out by Robertson Microlit Laboratories, Madison, NJ, USA. $PhN(H)C(O)CH_2SH$,[63] $[Tm^{But}]HgBr$,[28] $[Tm^{But}]HgEt$,[10] $[Tm^{But}]HgSPh$[10] and $[Tm^{But}]ZnSePh$[17] were synthesized as previously reported. ***CAUTION: All mercury compounds are toxic and appropriate safety precautions must be taken in handling these compounds***.

X-ray structure determinations

Single crystal X-ray diffraction data were collected on either a Bruker Apex II diffractometer or a Bruker P4 diffractometer equipped with a SMART CCD detector. Crystal data, data collection and refinement parameters are summarized in Table S1. The structures were solved using direct methods and standard difference map techniques, and were refined by full-matrix least-squares procedures on F^2 with SHELXTL (Version 6.10).[64]

Computational Details

All calculations were carried out using DFT as implemented in the Jaguar 6.0 suite of *ab initio* quantum chemistry programs.[65] Geometry optimizations were performed with the B3LYP density functional[66] and the 6-31G** (C, H, N, B, O, S), LAV3P (Zn, Hg, Se, Te) basis sets. The energies of the optimized structures (Table S2) were reevaluated by additional single point calculations on each optimized geometry using cc-pVTZ(-f) correlation consistent triple-ζ (C, H, N, B, O, S) and LAV3P (Zn, Hg, Se, Te) basis sets.

$[Tm^{But}]HgCl$

A mixture of $[Tm^{But}]K$ (500 mg, 0.968 mmol) and $HgCl_2$ (263 mg, 0.968 mmol) was treated with CH_2Cl_2 (10 mL). The resulting white slurry was stirred for a period of 30 minutes and filtered. The volatile components of the filtrate were removed *in vacuo* giving $[Tm^{But}]HgCl$ as a pale yellow solid (343 mg, 50%). ^1H NMR (C_6D_6): 1.44 [s, 27 H of $HB\{C_3N_2H_2[C(C\underline{H}_3)_3]S\}_3$], 4.8 [br, 1 H of $\underline{H}B\{C_3N_2H_2[C(CH_3)_3]S\}_3$], 6.36 [d, $^3J_{H\text{-}H} = 2$, 3 H of $HB\{C_3N_2\underline{H}_2[C(CH_3)_3]S\}_3$], 6.63 [d, $^3J_{H\text{-}H} = 2$, 3 H of $HB\{C_3N_2\underline{H}_2[C(CH_3)_3]S\}_3$. ^{13}C NMR (C_6D_6): 28.7 [9 C of $HB\{C_2N_2H_2[C(\underline{C}H_3)_3]CS\}_3$], 59.6 [3 C of $HB\{C_2N_2H_2[\underline{C}(CH_3)_3]CS\}_3$], 117.0 [3 C of $HB\{\underline{C}_2N_2H_2[C(CH_3)_3]CS\}_3$. IR Data (KBr pellet, cm^{-1}): 3157 (w), 3143 (w), 2977 (s), 2922 (m), 2884 (w), 2542 (m), 2407 (w), 1557 (s), 1481 (m), 1420 (vs), 1399 (m), 1360 (vs), 1305 (s), 1267 (m), 1229 (w), 1200 (vs), 1165 (vs), 1103 (s), 1063 (s), 1029 (w), 969 (w), 926 (m), 819 (m), 731 (vs), 689 (s), 643 (w), 635 (w). Mass spectrum: *m/z* = 679.22 $\{M - Cl\}^+$. Crystals suitable for X–ray diffraction were obtained from CH_2Cl_2.

Synthesis of $[Tm^{But}]HgSCH_2C(O)N(H)Ph$

(a) A solution of $PhN(H)C(O)CH_2SH$ (47 mg, 0.28 mmol) in EtOH (10 mL) was treated with Li (2 mg, 0.29 mmol) and stirred at room temperature for 3 hours. After this period, a solution of $[Tm^{But}]HgCl$ (200 mg, 0.28 mmol) in EtOH (20 mL) was added and the mixture was stirred for 1 day, resulting in the formation of a white precipitate. The mixture was filtered and the volatile components were removed from filtrate *in vacuo* to give $[Tm^{But}]HgSCH_2C(O)N(H)Ph$ as a white powder (160 mg, 68%). Crystals of composition $[Tm^{But}]HgSCH_2C(O)N(H)Ph$ suitable for X-ray diffraction were obtained from CH_3CN. Analysis calcd. $[Tm^{But}]HgSCH_2C(O)N(H)Ph$: C, 41.3%; H, 5.0%; N, 11.5%. Found: C, 41.4%; H, 5.0%; N, 11.5%. ^1H NMR (C_6D_6): 1.43 [s, 27 H of $HB\{C_3N_2H_2[C(C\underline{H}_3)_3]S\}_3$], 3.92 [d, 1 H part A of "AB" quartet, $^2J_{H\text{-}H} = 18$, $HgSC\underline{H}_2C(O)N(H)Ph$], 4.26 [d, 1 H part A of "AB" quartet, $^2J_{H\text{-}H} = 18$, $HgSC\underline{H}_2C(O)N(H)Ph$], 6.33 [d, $^3J_{H\text{-}H} = 2$, 3 H of $HB\{C_3N_2\underline{H}_2[C(CH_3)_3]S\}_3$], 6.63

[d, $^{3}J_{H-H}$ = 2, 3 H of HB{$C_3N_2\underline{H}_2[C(CH_3)_3]S\}_3$], 6.87 [m, 1 H, *p*-$HgSCH_2C(O)N(H)\underline{Ph}$], 7.92 [d, 2 H, $^{3}J_{H-H}$ = 8, *o*-$HgSCH_2C(O)N(H)\underline{Ph}$], 10.16 [br, 1 H, $HgSCH_2C(O)N(\underline{H})Ph$]. ^{13}C NMR ($C_6D_6$): 28.7 [9 C of HB{$C_2N_2H_2[C(\underline{C}H_3)_3]CS\}_3$], 59.4 [3 C of HB{$C_2N_2H_2[\underline{C}(CH_3)_3]CS\}_3$], 116.9 [3 C of HB{$\underline{C}_2N_2H_2[C(CH_3)_3]CS\}_3$], 119.5 [$HgSCH_2C(O)N(H)\underline{Ph}$], 122.8 [3 C of HB{$\underline{C}_2N_2H_2[C(CH_3)_3]CS\}_3$], 123.2 [$HgSCH_2C(O)N(H)\underline{Ph}$], 157.6 [3 C of HB {$C_2N_2H_2[C(CH_3)_3]\underline{C}S\}_3$]. IR Data (KBr pellet, cm^{-1}): 3317(w), 3170(w), 3142(w), 2964(m), 2923(w), 2411(m), 2234(w), 1673(s), 1652(w), 1645(w), 1634(w), 1622(w), 1600(m), 1568 (m), 1558(w), 1538(w), 1526(s), 1506(w), 1497(w), 1488(w), 1455(w), 1439(m), 1416(m), 1393(w), 1353(vs), 1302(w), 1259(w), 1228(w), 1192(s), 1173(s), 1125(w), 1094(w), 928(w), 887(w), 803(w), 754(m), 733(m), 723(m), 690(m), 640(w), 587(w), 550(w), 507(w), 465(w). Mass spectrum: *m/z* = 679.0 $\{M - PMA\}^+$.

(b) A mixture of $PhN(H)C(O)CH_2SH$ (44 mg, 0.26 mmol) and KH (21 mg, 0.53 mmol) was treated with THF (3 mL), stirred for 2 hours, and treated with [Tm^{Bu^t}]HgBr (200 mg, 0.26 mmol). The resulting mixture was stirred for 4 hours and filtered. The volatile components were removed from filtrate *in vacuo* to give [Tm^{Bu^t}]$HgSCH_2C(O)N(H)Ph$ as a white powder (85 mg, 38%).

(c) A solution of [Tm^{Bu^t}]HgEt (*ca*. 5 mg) in C_6D_6 was treated with $PhN(H)C(O)CH_2SH$ (*ca*. 5 mg) and monitored by ^{1}H NMR spectroscopy, thereby demonstrating the formation of [Tm^{Bu^t}]$HgSCH_2C(O)N(H)Ph$ and C_2H_6.

Synthesis of [Tm^{Bu^t}]HgSePh

A solution of [Tm^{Bu^t}]HgEt (100 mg, 0.141 mmol) in C_6H_6 (10 mL) was treated with PhSeH (40 μL, 0.375 mmol) in C_6H_6 (5 mL) and stirred for 16 hours. The volatile components were removed by lyophilization and the solid obtained was washed with pentane and dried *in vacuo* to give [Tm^{Bu^t}]HgSePh as a white powder (65 mg, 55% yield). Crystals of composition [Tm^{Bu^t}]HgSePh suitable for X-ray diffraction were obtained from Et_2O. Analysis calcd. [Tm^{Bu^t}]HgSePh: C, 38.9%; H, 4.7%; N, 10.1%. Found: C, 38.8%; H, 5.4%; N, 9.4%. ^{1}H NMR (C_6D_6): 1.45 [s, 27 H of HB{$C_3N_2H_2[C(C\underline{H}_3)_3]S\}_3$], 6.36 [d, $^{3}J_{H-H}$ = 2, 3 H of HB {$C_3N_2\underline{H}_2[C(CH_3)_3]S\}_3$], 6.69 [d, $^{3}J_{H-H}$ = 2, 3 H of HB{$C_3N_2\underline{H}_2[C(CH_3)_3]S\}_3$], 7.0 [m, 3 H of $TeC_6\underline{H}_5$], and 8.01 [d, $^{3}J_{H-H}$ = 6, 2 H of $TeC_6\underline{H}_5$]. ^{13}C NMR (C_6D_6): 28.8 [9 C of HB {$C_2N_2H_2[C(\underline{C}H_3)_3]CS\}_3$], 59.3 [3 C of HB{$C_2N_2H_2[\underline{C}(CH_3)_3]CS\}_3$], 116.7 [3 C of HB {$\underline{C}_2N_2H_2[C(CH_3)_3]CS\}_3$], 122.8 [3 C of HB{$\underline{C}_2N_2H_2[C(CH_3)_3]CS\}_3$], 124.7 [$HgSe\underline{Ph}$], 136.2, [$HgSe\underline{Ph}$], 158.1 [3 C of HB{$C_2N_2H_2[C(CH_3)_3]\underline{C}S\}_3$]. IR Data (KBr pellet, cm^{-1}): 3180 (w), 2973(m), 2361(m), 2344(m), 1578(m), 1561(m), 1474(m), 1459(w), 1415(m), 1397(w), 1355(vs), 1303(m), 1262(w), 1228(w), 1193(s), 1172(s), 1070(w), 1022(w), 820(w), 756(w), 729(m), 687(m). Mass spectrum: *m/z* = 833.4$\{M - 1\}^+$, 679.3 $\{M - SePh\}^+$.

Synthesis of [Tm^{Bu^t}]HgTePh

A mixture of [Tm^{Bu^t}]HgEt (25 mg, 0.04 mmol) and Ph_2Te_2 (7 mg, 0.02 mmol) was treated with C_6D_6 (1.0 mL), thereby resulting in the formation of a red solution. The reaction was monitored by ^{1}H NMR spectroscopy which revealed that the reaction proceeds to completion over a period of 1 day, after which period the mixture was filtered. The filtrate was allowed to stand at room temperature, thereby resulting in the formation of colorless crystals of composition [Tm^{Bu^t}]HgTePh•$0.5C_6H_6$ (*ca*. 5 mg). ^{1}H NMR (C_6D_6): 1.47 [s, 27 H of HB {$C_3N_2H_2[C(C\underline{H}_3)_3]S\}_3$], 4.8 [br, 1 H of $\underline{H}B\{C_3N_2H_2[C(CH_3)_3]S\}_3$], 6.53 [d, $^{3}J_{H-H}$ = 2, 3 H of HB{$C_3N_2\underline{H}_2[C(CH_3)_3]S\}_3$], 6.65 [d, $^{3}J_{H-H}$ = 2, 3 H of HB{$C_3N_2\underline{H}_2[C(CH_3)_3]S\}_3$], 6.9 [m, 2 H of $TeC_6\underline{H}_5$], 7.60 [d, $^{3}J_{H-H}$ = 8, 1 H of $TeC_6\underline{H}_5$], and 8.03 [d, $^{3}J_{H-H}$ = 8, 2 H of $TeC_6\underline{H}_5$].

Chalcogenolate transfer between [Tm^{But}]HgSCH$_2$C(O)N(H)Ph and [Tm^{But}]ZnSePh

(a) A solution of [Tm^{But}]HgSCH$_2$C(O)N(H)Ph in C_6D_6 (0.7 mL) was treated with incremental portions of [Tm^{But}]ZnSePh and the reaction was monitored by ^{1}H NMR spectroscopy which demonstrated conversion to [Tm^{But}]ZnSCH$_2$C(O)N(H)Ph and [Tm^{But}]HgSePh.

(b) A mixture of [Tm^{But}]ZnSCH$_2$C(O)N(H)Ph and [Tm^{But}]HgSePh was treated with C_6D_6 (0.7 mL). The sample was examined by ^{1}H NMR spectroscopy, which demonstrated that the mixture contained only [Tm^{But}]ZnSCH$_2$C(O)N(H)Ph and [Tm^{But}]HgSePh in the ratio *ca*. 1:5, with there being no discernible formation of [Tm^{But}]HgSCH$_2$C(O)N(H)Ph and [Tm^{But}]ZnSePh. On the basis that a *ca*. 3:100 ratio of [Tm^{But}]HgSCH$_2$C(O)N(H)Ph to {[Tm^{But}]ZnSCH$_2$C(O)N(H)Ph + [Tm^{But}]HgSePh} should be observable, an upper limit for the equilibrium constant is estimated to be $< 6.6 \times 10^{-3}$; correspondingly, a lower limit for the reaction between [Tm^{But}]ZnSCH$_2$C(O)N(H)Ph and [Tm^{But}]HgSePh is > 150.

Chalcogenolate transfer between [Tm^{But}]HgSCH$_2$C(O)N(H)Ph and [Tm^{But}]ZnSPh

A mixture of [Tm^{But}]HgSPh and [Tm^{But}]ZnSCH$_2$C(O)N(H)Ph was treated with CD_2Cl_2 (0.7 mL) and mesitylene (5 μL). The reaction was monitored by ^{1}H NMR spectroscopy, thereby demonstrating the formation of an equilibrium mixture with [Tm^{But}]HgSCH$_2$C(O)N(H)Ph and [Tm^{But}]ZnSPh. The sample was allowed to equilibrate at room temperature for 1 day and the equilibrium constant was obtained by analysis of the NMR spectrum. The reaction was performed several times with different amounts of reactants and the average equilibrium constant for formation of [Tm^{But}]HgSCH$_2$C(O)N(H)Ph and [Tm^{But}]ZnSPh from [Tm^{But}]HgSPh and [Tm^{But}]ZnSCH$_2$C(O)N(H)Ph is 1.3(4).

Supplementary Material

Refer to Web version on PubMed Central for supplementary material.

Acknowledgments

We thank the National Institutes of Health (GM046502) and the National Science Foundation (CHE-0749674) for support of this research. The National Science Foundation (CHE-0619638) is thanked for acquisition of an X–ray diffractometer.

Supporting Information Available: Tables of crystallographic data, CIF files and cartesian coordinates for geometry optimized structures. This material is available free of charge *via* the Internet at http://pubs.acs.org.

References

1. (a) Clarkson TW, Magos L. Crit Rev Toxicol 2006;36:609–662. [PubMed: 16973445] (b) Mutter J, Naumann J, Guethlin C. Crit Rev Toxicol 2007;37:537–549. [PubMed: 17661216] (c) Clarkson TW. Env Health Persp Suppl 2002;110:11–23. (d) Clarkson TW. Crit Rev Clin Lab Sci 1997;34:369–403. [PubMed: 9288445] (e) Langford NJ, Ferner RE. J Human Hypertension 1999;13:651–656. (f) Boening DW. Chemosphere 2000;40:1335–1351. [PubMed: 10789973] (g) Magos L. Metal Ions in Biological Systems 1997;34:321–370. [PubMed: 9046575] (h) Hutchison AR, Atwood DA. J Chem Crystallogr 2003;33:631–645. (i) Alessio L, Campagna M, Lucchini R. Am J Ind Med 2007;50:779–787. [PubMed: 17918211] (j) Clarkson TW, Vyas JB, Ballatorl N. Am J Ind Med 2007;50:757–764. [PubMed: 17477364] (k) Risher JF, De Rosa CT. J Env Health 2007;70:9–16. [PubMed: 18044248] (l) Onyido I, Norris AR, Buncel E. Chem Rev 2004;104:5911–5929. [PubMed: 15584692] (m) Ozuah PO. Curr Probl Pediatr 2000;30:91–99. [PubMed: 10742922]
2. Tai HC, Lim C. J Phys Chem A 2006;110:452–462. [PubMed: 16405317]
3. (a) Rooney JPK. Toxicology 2007;234:145–156. [PubMed: 17408840] (b) Guzzi G, La Porta CAM. Toxicology 2008;244:1–12. [PubMed: 18077077]

4. (a) Prince RC, Gailer J, Gunson DE, Turner RJ, George GN, Pickering IJ. J Inorg Biochem 2007;101:1891–1893. [PubMed: 17644180] (b) Gailer J. Coord Chem Rev 2007;251:234–254. (c) Gailer J. Appl Organometal Chem 2002;16:701–707. (d) Cuvin-Aralar MLA, Furness RW. Ecotoxicol Env Safety 1991;21:348–364. [PubMed: 1868791] (e) Yang DY, Chen YW, Gunn JM, Belzile N. Selenium and mercury in organisms: Interactions and mechanisms. Environ Rev 2008;16:71–92. (f) Ikemoto T, Kunito T, Tanaka H, Baba N, Miyazaki N, Tanabe S. Arch Environ Cont Toxicol 2004;47:402–413. (g) Magos L, Webb M, Clarkson TW. Crit Rev Toxicol 1980;8:1–42. [PubMed: 7002474] (h) Soldin OP, O'Mara DM, Aschner M. Biol Trace Elem Res 2008;126:1–12. [PubMed: 18716716] (i) Whanger PD. J Trace Elem Electrolytes Health Dis 1992;6:209–221. [PubMed: 1304229] (j) Kaur P, Evje L, Aschner M, Syversen T. Toxicol Vitro 2009;23:378–385. (k) Peterson SA, Ralston NVC, Peck DV, Van Sickle J, Robertson JD, Spate VL, Morris JS. Environ Sci Technol 2009;43:3919–3925. [PubMed: 19544908] (l) Seppänen K, Soininen P, Salonen JT, Lötjönen S, Laatikainen R. Biol Trace Elem Res 2004;101:117–132. [PubMed: 15557676] (m) Ralston NVC, Ralston CR, Blackwell JL III, Raymond LJ. Neurotoxicology 2008;29:802–811. [PubMed: 18761370]
5. (a) Köhrle J. Biochimie 1999;81:527–533. [PubMed: 10403185] (b) Reddy CC, Massaro EJ. Fundam Appl Toxicol 1983;3:431–436. [PubMed: 6357927] (c) Frost DV, Lish PM. Ann Rev Pharmacol Toxicol 1975;15:259–284.
6. (a) Papp LV, Lu J, Holmgren A, Khanna KK. Antioxidants & Redox Signalling 2007;9:775–806. (b) Jacob C, Giles GI, Giles NM, Sies H. Angew Chem Int Ed Engl 2003;42:4742–4758. [PubMed: 14562341] (c) Wessjohann LA, Schneider A, Abbas M, Brandt W. Biol Chem 2007;388:997–1006. [PubMed: 17937613] (d) Roy G, Sarma BK, Phadnis PP, Mugesh G. J Chem Sci 2005;117:287–303.
7. (a) Falnoga I, Tusek-Znidaric M. Biol Trace Elem Res 2007;119:212–220. [PubMed: 17916944] (b) Falnoga I, Tusek-Znidaric M, Stegnar P. BioMetals 2006;19:283–294. [PubMed: 16799866] (c) Sasakura C, Suzuki KT. J Inorg Biochem 1998;71:159–162. [PubMed: 9833321]
8. (a) Ralston NVC, Ralston CR, Blackwell JL III, Raymond LJ. Neurotoxicology 2008;29:802–811. [PubMed: 18761370] (b) Carvalho CML, Chew EH, Hashemy SI, Lu J, Holmgren A. J Biol Chem 2008;283:11913–11923. [PubMed: 18321861]
9. (a) Potter S, Matrone G. J Nutr 1974;104:638–647. [PubMed: 4856782] (b) Magos L, Webb M. CRC Crit Rev Toxicol 1980;8:1–42.
10. Melnick JG, Parkin G. Science 2007;317:225–227. [PubMed: 17626880]
11. (a) Parkin G. New J Chem 2007;31:1996–2014. (b) Parkin G. Chem Rev 2004;104:699–767. [PubMed: 14871139] (c) Parkin G. Chem Commun 2000:1971–1985.
12. For other representative studies, see: (a) Rabinovich D. Struct Bond 2006;120:143–162. (b) Vahrenkamp H. Dalton Trans 2007:4751–4759. [PubMed: 17955125]
13. The structure of [Tm^{Bu^t}]HgSPh has also been obtained at a higher temperature (243 K) than described here (170 K). See: Melnick JG, Parkin G. Science 2007;317:225–227. reference 10. [PubMed: 17626880]
14. Christou G, Folting K, Huffman JC. Polyhedron 1984;3:1247–1253.
15. Lang ES, Dias MM, Abram U, Vázquez-López EM. Z Anorg Allg Chem 2000;626:784–788.
16. Behrens U, Hoffmann K, Klar G. Chem Ber 1977;110:3672–3677.
17. Melnick JG, Docrat A, Parkin G. Chem Commun 2004:2870–2871.
18. Melnick JG, Parkin G. Dalton Trans 2006:4207–4210. [PubMed: 16932812]
19. Cordero B, Gómez V, Platero-Prats AE, Revés M, Echeverría J, Cremades E, Barragán F, Alvarez S. Dalton Trans 2008:2832–2838. [PubMed: 18478144]
20. Haaland A. J Mol Struct 1983;97:115–128.
21. Pyykkö P. Chem Rev 1988;88:563–594.
22. For the same reasons, Au is also smaller than its lighter congener, Ag. See, for example: (a) Bayler A, Schier A, Bowmaker GA, Schmidbaur H. J Am Chem Soc 1996;118:7006–7007. (b) Tripathi UM, Bauer A, Schmidbaur H. J Chem Soc Dalton Trans 1997:2865–2868. (c) Bruce MI, Williams ML, Patrick JM, Skelton BW, White AH. J Chem Soc Dalton Trans 1986:2557–2567. (d) Fujisawa K, Imai S, Moro-oka Y. Chem Lett 1998:167–168. (e) Omary MA, Rawashdeh-Omary MA, Gonser MWA, Elbjeirami O, Grimes T, Cundari TR, Diyabalanage HVK, Gamage CSP, Dias HVR. Inorg Chem 2005;44:8200–8210. [PubMed: 16270956]

23. It is also worth noting that Ga and Al have very similar sizes due the scandide contraction, a main group counterpart of the lanthanide contraction that rationalizes the similarity of the sizes of the 2^{nd} and 3^{rd} row transition metals. See: Dowling CM, Parkin G. Polyhedron 1999;18:3567–3571.
24. Zhu Z, Brynda M, Wright RJ, Fischer RC, Merrill WA, Rivard E, Wolf R, Fettinger JC, Olmstead MM, Power PP. J Am Chem Soc 2007;129:10847–10857. [PubMed: 17691782]
25. Lutz M, Findeis B, Haukka M, Graff R, Pakkanen TA, Gade LH. Chem Eur J 2002;8:3269–3276.
26. Fujisawa K, Matsunaga Y, Ibi N, Amir N, Miyashita Y, Okamoto KI. Bull Chem Soc Jpn 2006;79:1894–1896.
27. Cassidy I, Garner M, Kennedy AR, Potts GBS, Reglinski J, Slavin PA, Spicer MD. Eur J Inorg Chem 2002:1235–1239.
28. White JL, Tanski JM, Rabinovich D. Dalton Trans 2002;15:2987–2991.
29. Minoura M, Landry VK, Melnick JG, Pang K, Marchiò L, Parkin G. Chem Commun 2006:3990–3992.
30. Cambridge Structural Database (Version 5.29). *3D Search and Research Using the Cambridge Structural Database*, Allen FH, Kennard O. Chemical Design Automation News 1993;8(1):1, 31–37.
31. Cameron AF, Forrest KP, Ferguson G. J Chem Soc (A) 1971:1286–1289.
32. Kessler JM, Reeder JH, Vac R, Yeung C, Nelson JH, Frye JS, Alcock NW. Magn Reson Chem 1991;29:S94–104.
33. Lobana TS, Sandhu MK, Snow MR, Tiekink ERT. Acta Cryst 1988;C44:179–181.
34. Fälth L. Chem Scripta 1976;9:71–73.
35. Although it is well known that M←L dative bonds are very sensitive to the environment of the acceptor atom (Haaland A. Angew Chem Int Ed Engl 1989;28:992–1007.), the observation of two trends in bond lengths for both [Tm^{But}]MEPh and $(Ph_3P)_2MX_2$ cannot simply be ascribed to the normal covalent versus dative covalent nature of the metal–ligand interactions because these two series of compounds exhibit opposite trends. For example, while the Cd–Cl bond of $(Ph_3P)_2CdCl_2$ is shorter than the Hg–Cl bond of $(Ph_3P)_2HgCl_2$, the Hg– EPh bonds of [Tm^{But}]HgEPh are shorter than the Cd–EPh bonds of [Tm^{But}]CdEPh. Correspondingly, while the dative Cd–P bonds of $(Ph_3P)_2CdCl_2$ are longer than the Hg–P bonds of $(Ph_3P)_2HgCl_2$, the Cd–[Tm^{But}] bonds of [Tm^{But}]CdEPh (which possess a 2/3 dative component) are shorter than the Hg–[Tm^{But}] bonds of [Tm^{But}]HgEPh
36. Using the standard deviation as an indication of the experimental error in the measurement of the M–E bond length, the errors associated with the differences in Hg–EPh and Cd–EPh bond lengths (Table 1) are estimated to be 0.010 ± 0.001 (S), 0.035 ± 0.001 (Se), and 0.057 ± 0.014 (Te), while the differences in Hg–EPh and Zn–EPh bond lengths are estimated to be 0.177 ± 0.001 (S), 0.130 ± 0.001 (Se), 0.085 ± 0.014 (Te).
37. Chalcogen covalent radii: S (1.05 Å), Se (1.20 Å), Te (1.38 Å). See: Cordero B, Gómez V, Platero-Prats AE, Revés M, Echeverría J, Cremades E, Barragán F, Alvarez S. Dalton Trans 2008:2832–2838. reference 19. [PubMed: 18478144]
38. It must be emphasized that this description of the structural changes are relative to the sulfur system and are not absolute. If one were to normalize all values relative to the tellurium system, one would simply conclude that the M–SPh and M–SePh bonds are longer than predicted on the basis of the change in covalent radii of the chalcogens. These are merely different ways of describing the same situation, *i.e.* the M–EPh bond lengths do not scale equally with the covalent radii of the chalcogens, with the M–TePh bonds being relatively shorter and the M– SPh bonds being relatively longer than expected.
39. Howard WA, Trnka TM, Parkin G. Inorg Chem 1995;34:5900–5909.
40. Gaunt AJ, Reilly SD, Enriquez AE, Scott BL, Ibers JA, Sekar P, Ingram KIM, Kaltsoyannis N, Neu MP. Inorg Chem 2008;47:29–41. [PubMed: 18020446]
41. Hillier AC, Liu SY, Sella A, Elsegood MRJ. Inorg Chem 2000;39:2635–2644. [PubMed: 11197020]
42. Although the qualitative terms thiophilic, selenophilic and tellurophilic (and, more generally, chalcogenophilic) strictly relate to thermodynamics of the M–E interactions, here we are using perturbations in M–E bond lengths to infer differences in chalcogenophilicity.

43. Melnick JG, Zhu G, Buccella D, Parkin G. J Inorg Biochem 2006;100:1147–1154. [PubMed: 16516971]
44. Pauling, L. The Nature of The Chemical Bond. 3rd. Cornell University Press; Ithaca, NY: 1960. p. 93
45. Wu KY, Hsieh CC, Horng YC. J Organomet Chem 2009;694:2085–2091.
46. Baba K, Okamura T, Yamamoto H, Yamamoto T, Ueyama N. Inorg Chem 2008;47:2837–2848. [PubMed: 18330987]
47. Capps KB, Wixmerten B, Bauer A, Hoff CD. Inorg Chem 1998;37:2861–2864.
48. McDonough JE, Weir JJ, Sukcharoenphon K, Hoff CD, Kryatova OP, Rybak-Akimova EV, Scott BL, Kubas GJ, Mendiratta A, Cummins CC. J Am Chem Soc 2006;128:10295–10303. [PubMed: 16881661]
49. González-Blanci O, Branchadell V, Monteyne K, Ziegler T. Inorg Chem 1998;37:1744–1748.
50. McDonough JE, Mendiratta A, Curley JJ, Fortman GC, Fantasia S, Cummins CC, Rybak-Akimova EV, Nolan SP, Hoff CD. Inorg Chem 2008;47:2133–2141. [PubMed: 18260626]
51. (a) Levason W, Orchard SD, Reid G. Coord Chem Rev 2002;225:159–199. (b) Hope EG, Levason W. Coord Chem Rev 1993;122:109–170. (c) Schumann H, Arif AM, Rheingold AL, Janiak C, Hoffmann R, Kuhn N. Inorg Chem 1991;30:1618–1625.
52. Arnold AP, Tan KS, Rabenstein DL. Inorg Chem 1986;25:2433–2437.
53. Furthermore, the formation constant for MeHgSeCN is greater than that for MeHgSCN. See: Rabenstein DL, Tourangeau MC, Evans CA. Can J Chem 1976;54:2517–2525.
54. (a) Sugiura Y, Tamai Y, Tanaka H. Bioinorg Chem 1978;9:167–180. [PubMed: 698281] (b) Sugiura Y, Hojo Y, Tamai Y, Tanaka H. J Am Chem Soc 1976;98:2339–2340. [PubMed: 1254870]
55. (a) Carty AJ, Malone SF, Taylor NJ, Canty AJ. J Inorg Biochem 1983;18:291–300. (b) Canty AJ, Carty AJ, Malone SF. J Inorg Biochem 1983;19:133–142. (c) Carty AJ, Malone SF, Taylor NJ. J Organomet Chem 1979;172:201–211.
56. Ahrland S, Chatt J, Davies NR. Quart Rev 1958;12:265–276.
57. (a) Pearson RG. J Am Chem Soc 1963;85:3533–3539.(b) Pearson, RG. Chemical Hardness: Applications from Molecules to Solids. Wiley-VCH; New York: 1997.
58. Alderighi L, Gans P, Midollini S, Vacca A. Inorg Chim Acta 2003;356:8–18.
59. Blanusa M, Varnai VM, Piasek M, Kostial K. Curr Med Chem 2005;12:2771–2794. [PubMed: 16305472]
60. (a) Aposhian HV, Maiorino RM, Gonzalez-Ramirez D, Zuniga-Charles M, Xu Z, Hurlbut KM, Junco-Munoz P, Dart RC, Aposhian MM. Toxicol 1995;97:23–38. (b) Risher JF, Amler SN. NeuroToxicol 2005;26:691–699. (c) Baum CR. Curr Opin Ped 1999;11:265–8. (d) Aaseth J, Jacobsen D, Andersen O, Wickstrøm E. Analyst 1995;120:853–854. [PubMed: 7741240] (e) Bridges CC, Joshee L, Zalups RK. J Pharmacol Expt Therapeut 2008;324:383–390. (f) Domingo JL. Reprod Toxicol 1995;9:105–113. [PubMed: 7795320]
61. Gottlieb HE, Kotlyar V, Nudelman A. J Org Chem 1997;62:7512–7515. [PubMed: 11671879]
62. “CIL NMR Solvent Data Chart”, Cambridge Isotope Laboratories, Inc., Andover, MA 01810-5413, USA.
63. Bhandari CS, Sogani NC, Mahnot US. J Fur Praktische Chemie 1971;313:849–854.
64. (a) Sheldrick, GM. SHELXTL, An Integrated System for Solving, Refining and Displaying Crystal Structures from Diffraction Data. University of Göttingen; Göttingen, Federal Republic of Germany: 1981. (b) Sheldrick GM. Acta Cryst 2008;A64:112–122.
65. Jaguar 6.0, Schrödinger, LLC, New York, NY.
66. (a) Becke AD. J Chem Phys 1993;98:5648–5652. (b) Becke AD. Phys Rev A 1988;38:3098–3100. [PubMed: 9900728] (c) Lee CT, Yang WT, Parr RG. Phys Rev B 1988;37:785–789. (d) Vosko SH, Wilk L, Nusair M. Can J Phys 1980;58:1200–1211.(e) Slater, JC. The Self-Consistent Field for Molecules and Solids. Vol. 4. McGraw-Hill; New York: 1974. Quantum Theory of Molecules and Solids.

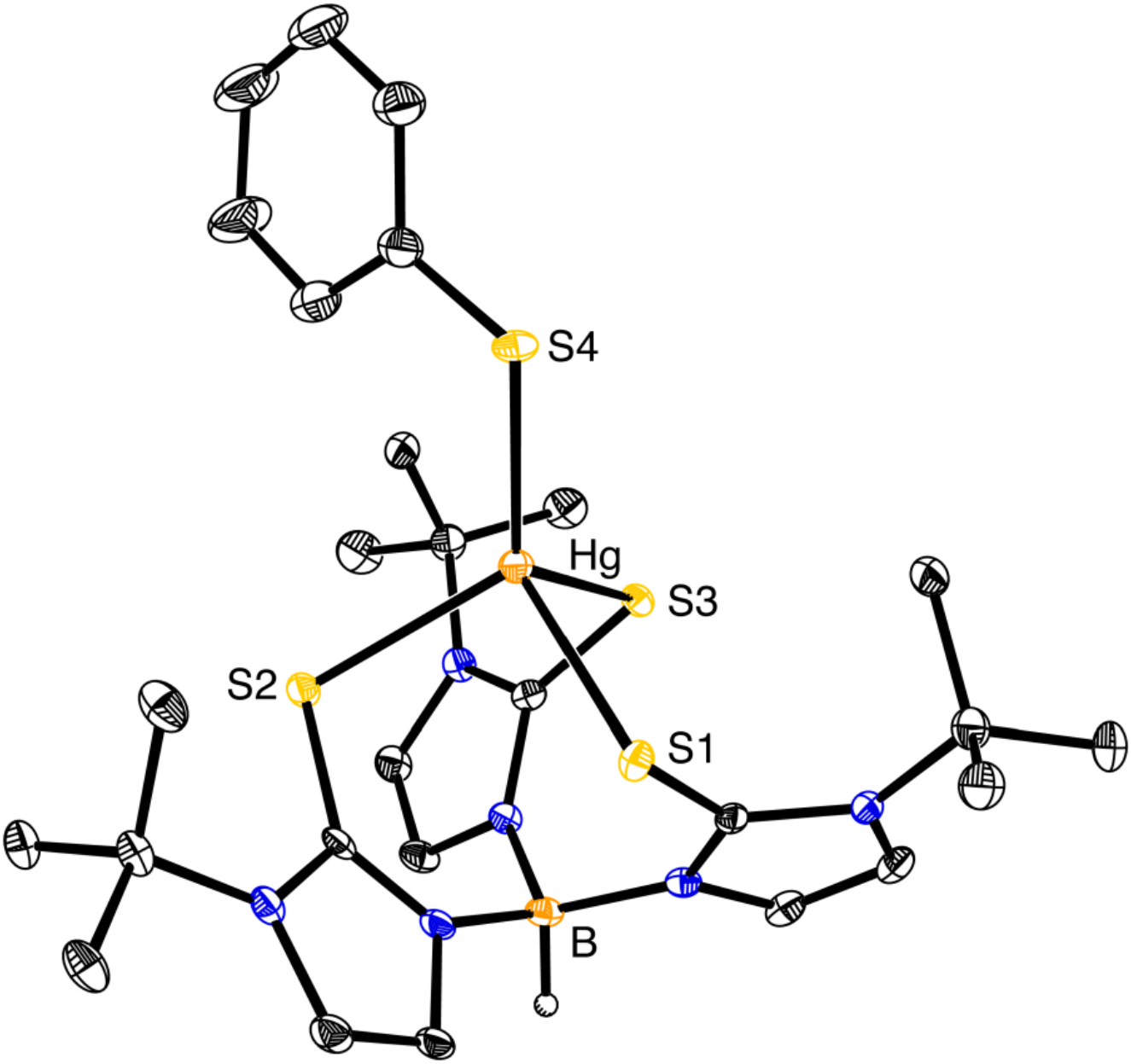

Figure 1.
Molecular structure of [Tm$^{Bu^t}$]HgSPh.

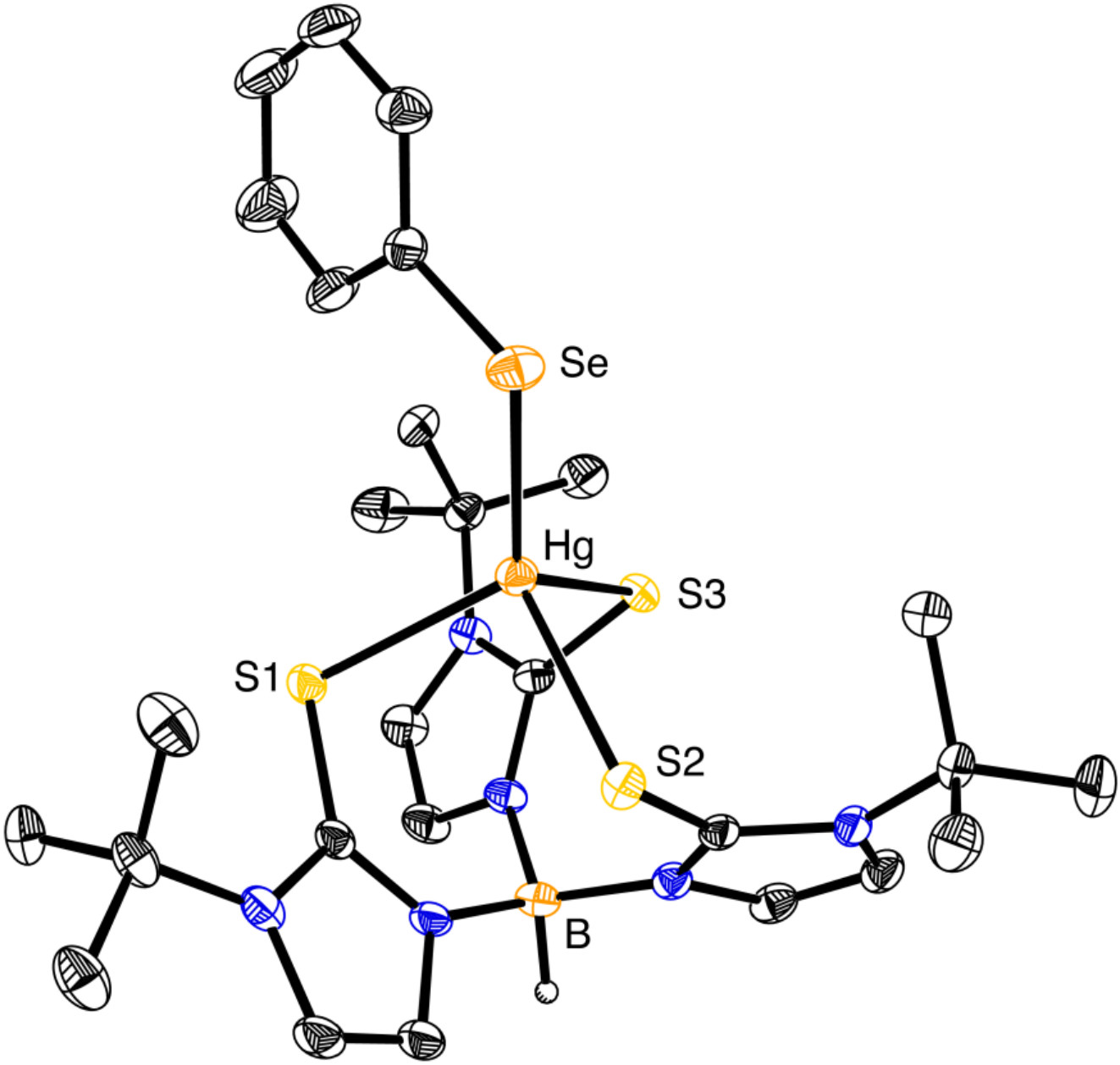

Figure 2.
Molecular structure of [Tm^{But}]HgSePh.

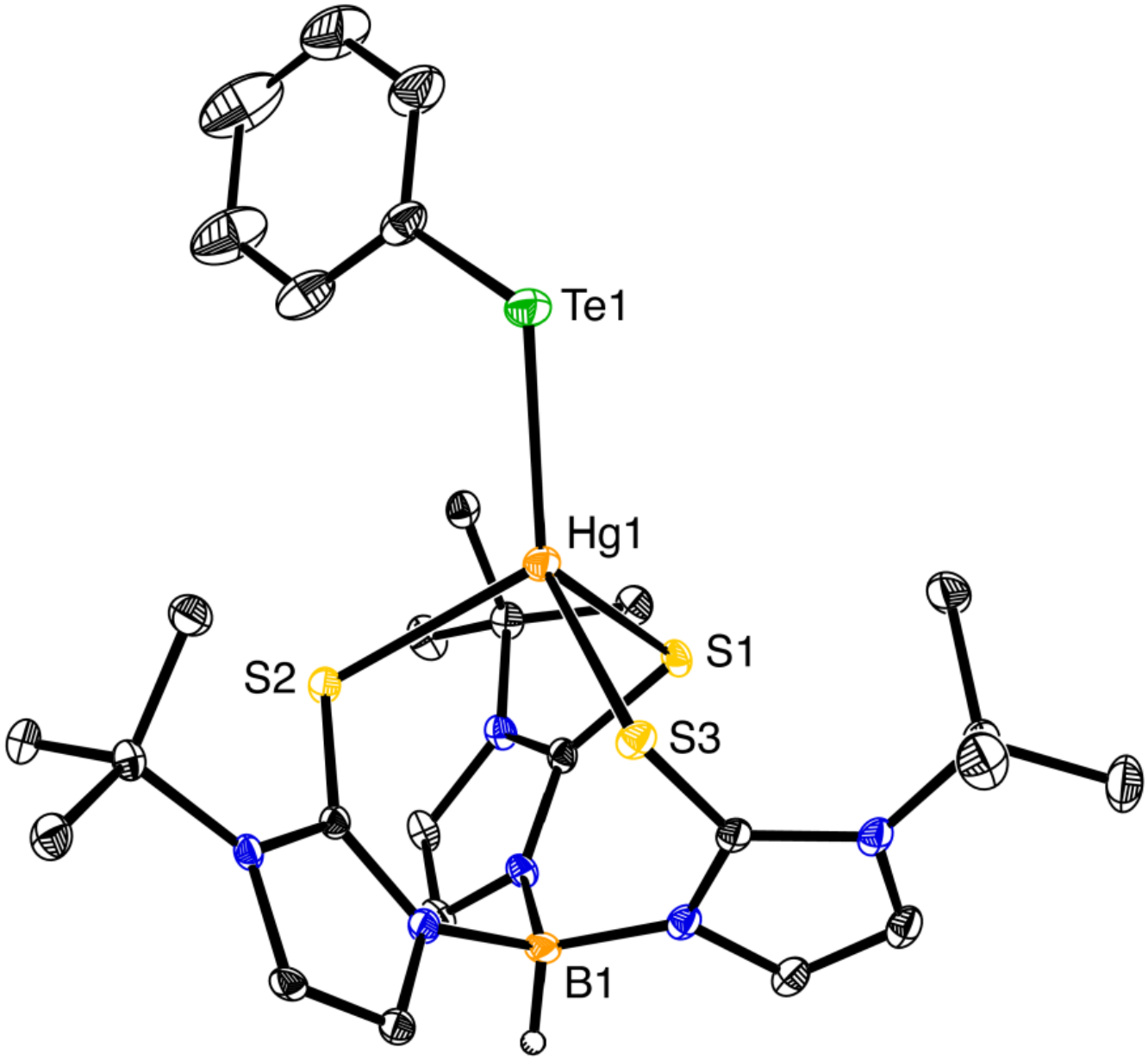

Figure 3.
Molecular structure of [Tm^{Bu}]HgTePh.

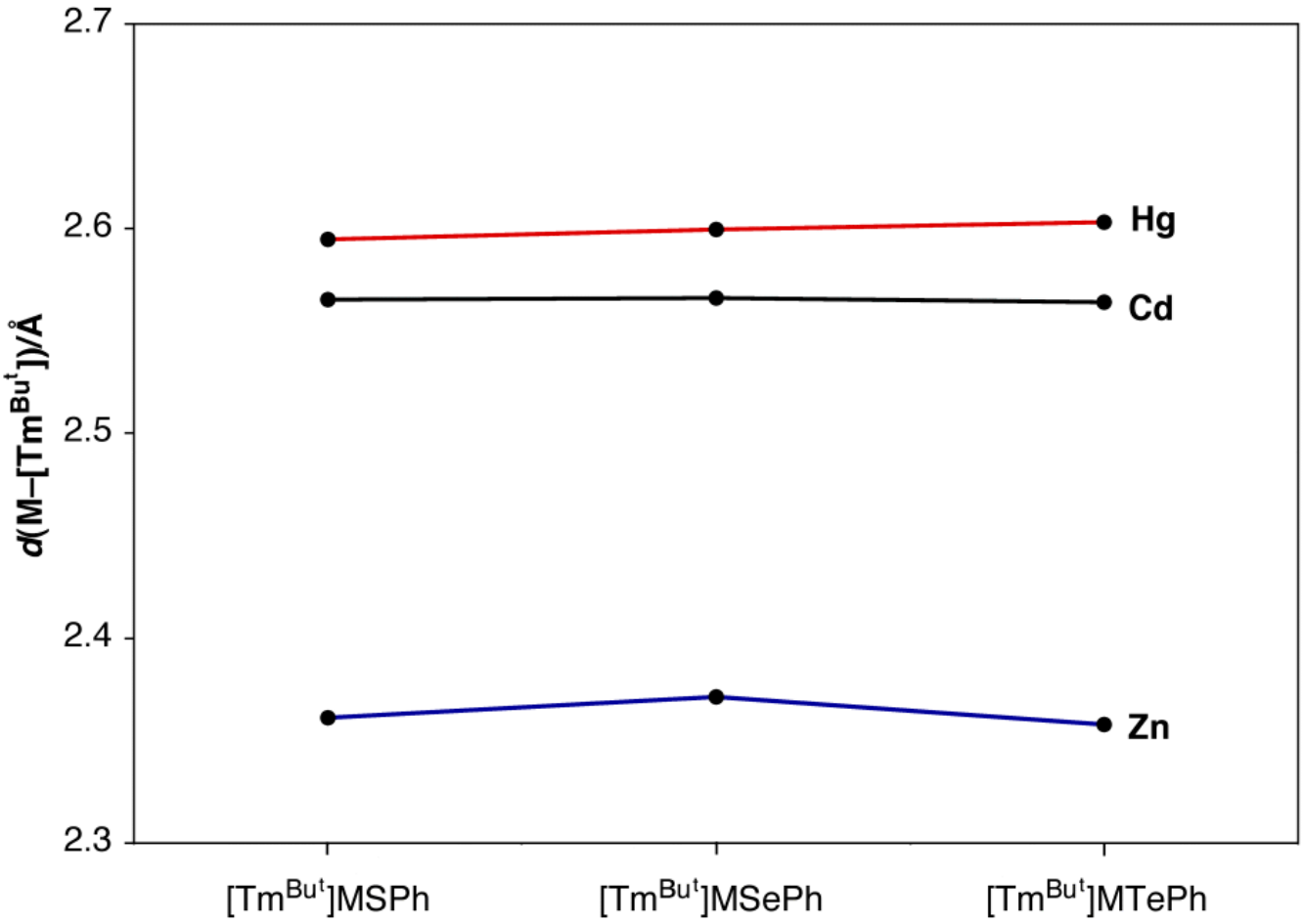

Figure 4.
Variation of M–S bond lengths involving the [Tm^{But}] ligand.

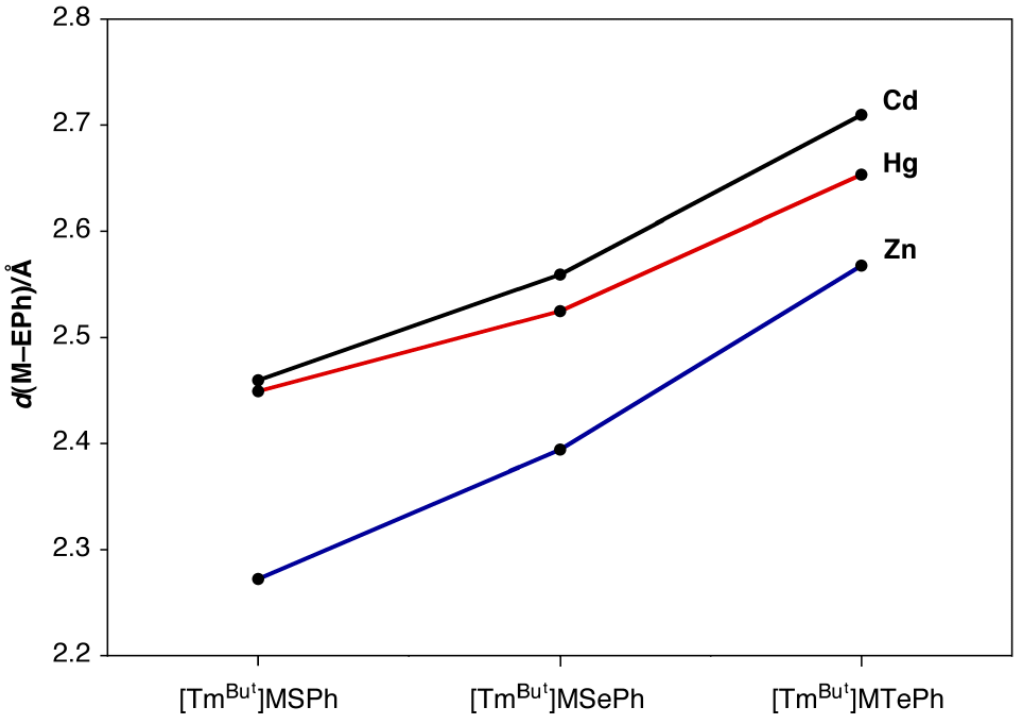

Figure 5.
Variation of M–EPh bond lengths.

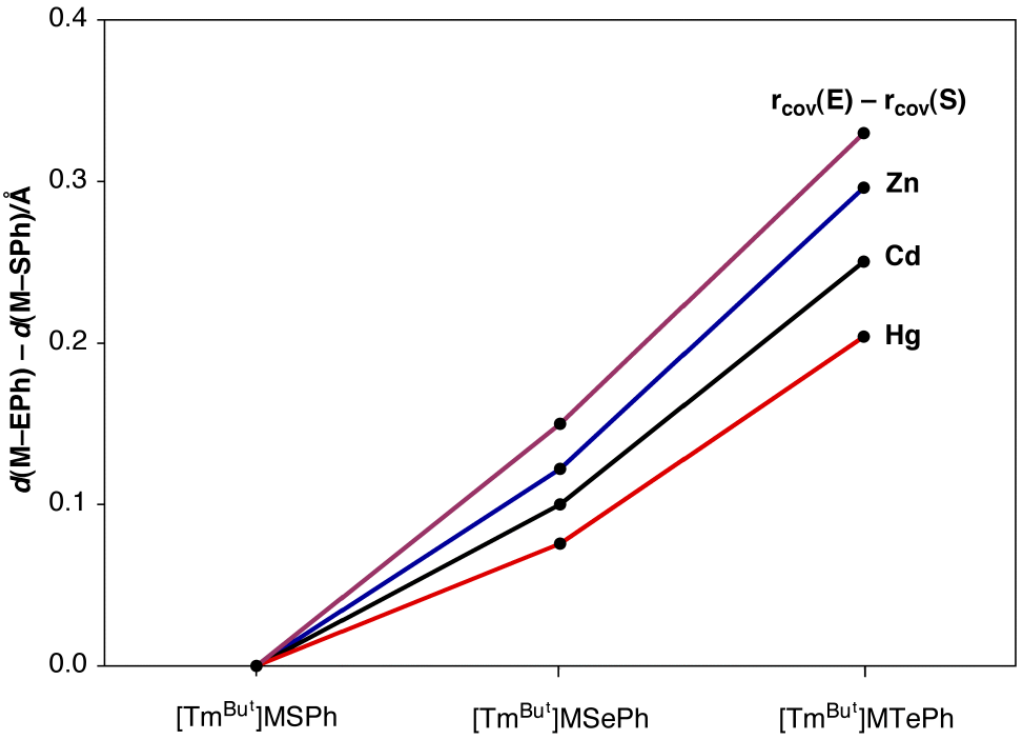

Figure 6.
Relative M–EPh bond lengths and the values predicted on the basis of the covalent radii of S, Se, Te.

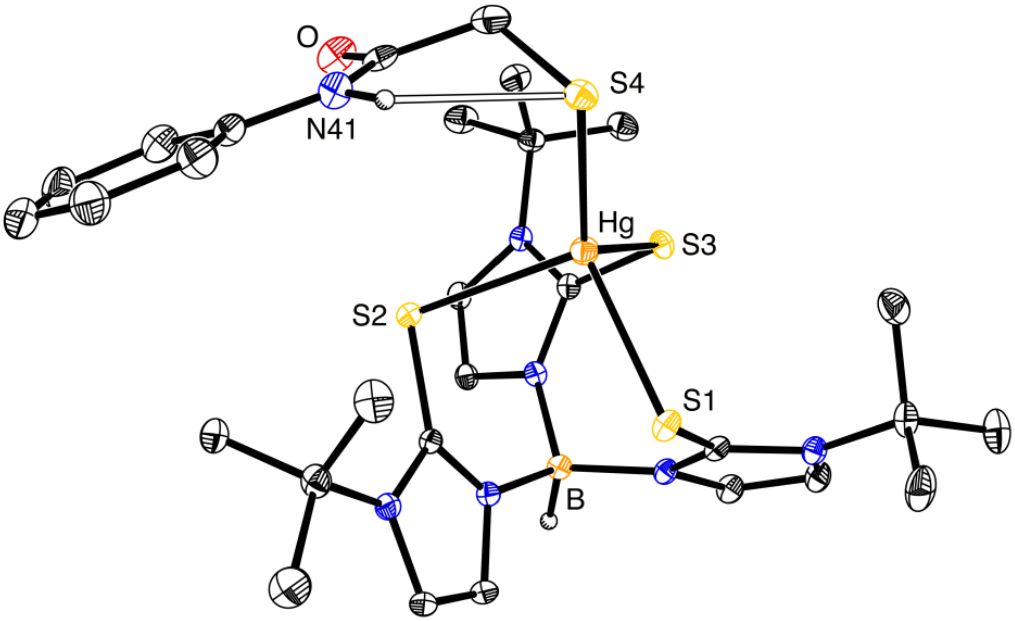

Figure 7.
Molecular structure of [Tm$^{Bu^t}$]HgSCH$_2$C(O)N(H)Ph.

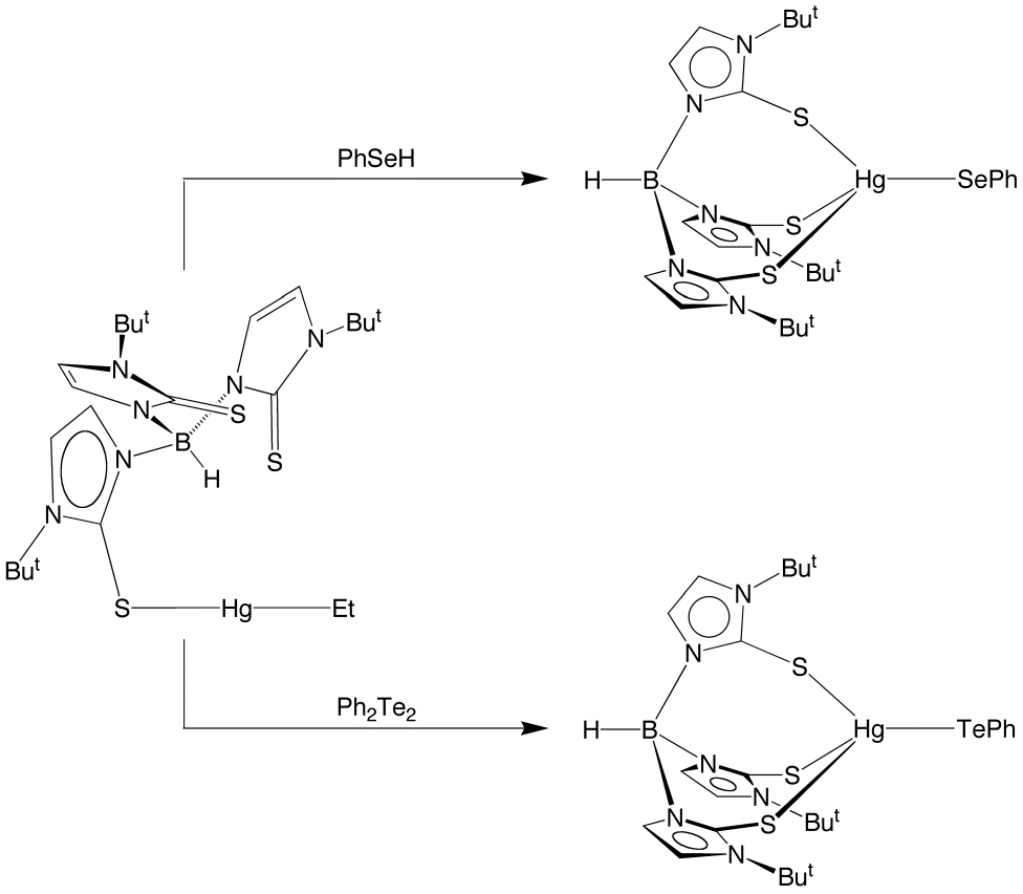

Scheme 1.

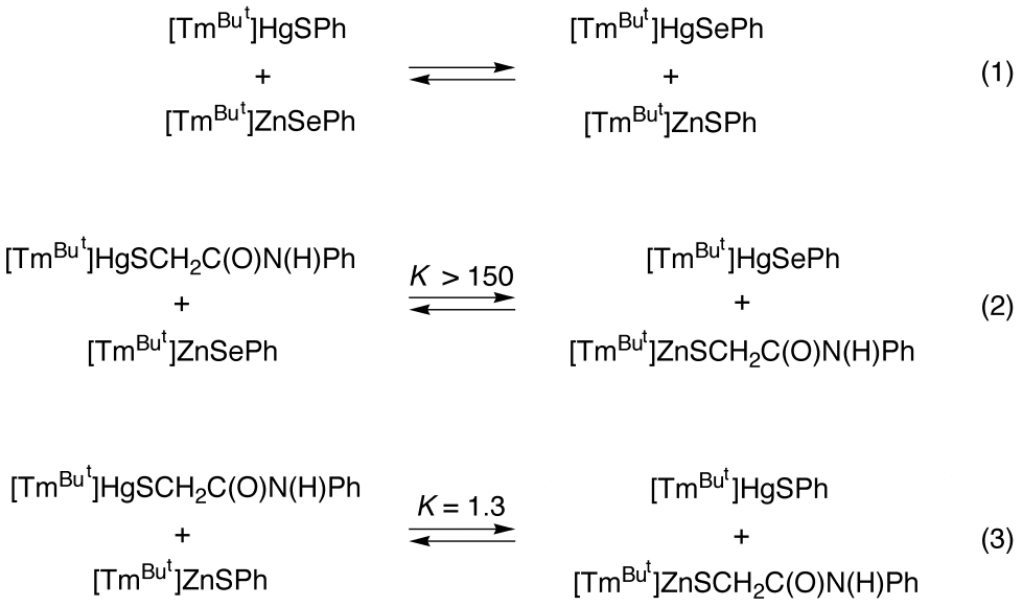

Scheme 2.

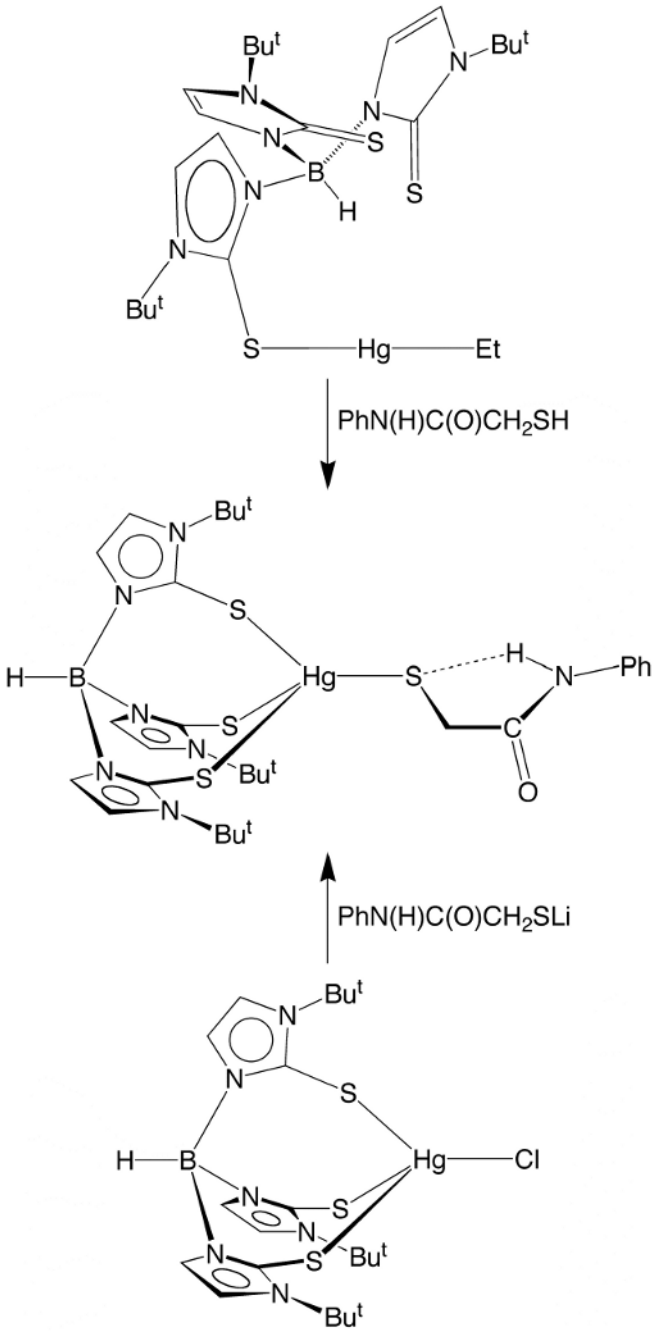

Scheme 3.

Table 1

M–EPh and M–[Tm$^{Bu^t}$] bond lengths (Å) for [Tm$^{Bu^t}$]MEPh (E = S, Se, Te).

	[Tm^{Bu}]MSPh		**[Tm^{Bu}]MSePh**		**[Tm^{Bu}]MTePh**	
	M–SPh	M-[Tm$^{Bu^t}$]$_{av}$	M–SePh	M-[Tm$^{Bu^t}$]$_{av}$	M–TePh	M-[Tm$^{Bu^t}$]$_{av}$
Zn[a]	2.272(1)	2.361[15]	2.394(1)	2.371[11]	2.568(1)	2.358[7]
Cd[b]	2.4595(7)	2.565[12]	2.5595(5)	2.566[9]	2.7097(5)	2.564[11]
Hg	2.449(1)[c]	2.594[19][c]	2.5244(4)[c]	2.600[20][c]	2.653[14][c,d]	2.602[18][c,e]

[(a)] reference 10b;

[(b)] reference 18;

[(c)] this work;

[(d)] average values for two molecules with individual bond lengths of 2.6630(7) and 2.6425(7) Å;

[(e)] average values for two molecules. Values in square brackets are standard deviations from multiple measurements.

Table 2

Comparison of Hg–X and Cd–X bond lengths from the literature.

	d(Hg–X)$_{av}$/Å	d(Cd–X)$_{av}$/Å	d(Hg–X) – d(Cd–X)	References
[Tm$^{Bu^t}$]MSPh (X = SPh)	2.449	2.460	−0.011	this work, 18
[Tm$^{Bu^t}$]MSPh (X = [Tm$^{Bu^t}$])	2.594	2.565	0.029	this work, 18
[Tm$^{Bu^t}$]MSePh (X = SePh)	2.524	2.560	−0.036	this work, 18
[Tm$^{Bu^t}$]MSePh (X = [Tm$^{Bu^t}$])	2.600	2.566	0.034	this work, 18
[Tm$^{Bu^t}$]MTePh (X = TePh)	2.653	2.710	−0.147	this work, 18
[Tm$^{Bu^t}$]MTePh (X = [Tm$^{Bu^t}$])	2.602	2.564	0.038	this work, 18
ArM–MAr Ar = C_6H_3-2,6-(C_6H_3-2,6-Pr$^i_2$)$_2$	2.574	2.626	−0.052	24
[MeSi{SiMe$_2$N(p-Tol)}$_3$Sn]$_2$M	2.650	2.676	−0.026	25
M(CH$_3$)$_2$	2.094	2.112	−0.018	20
[Tp^{Pri2}]MCl	2.301	2.332	−0.031	25
[Tse^{Mes}]MI	2.696	2.723	−0.027	29
[Tm^{Me}]MBr	2.564	2.567	−0.003	27
[Tm$^{Bu^t}$]MBr	2.533	2.536	−0.003	28
[MCl$_4$]$^{2-}$	2.487	2.458	0.029	30
[MBr$_4$]$^{2-}$	2.608	2.585	0.023	30
[MI$_4$]$^{2-}$	2.784	2.779	0.006	30
(Ph$_3$P)$_2$MCl$_2$ (X = Cl)	2.498	2.472	0.026	31, 33
(Ph$_3$P)$_2$MCl$_2$ (X = P)	2.518	2.634	−0.116	31, 33
(Ph$_3$P)$_2$MI$_2$ (X = Cl)	2.748	2.728	0.020	32, 34
(Ph$_3$P)$_2$MI$_2$ (X = P)	2.566	2.642	−0.076	32, 34

Table 3

DFT heterolytic $[Tm^{Bu^t}]HgER$ bond dissociation enthalpies (kcal mol^{-1})[a] for $[Tm^{Bu^t}]HgER \rightarrow \{[Tm^{Bu^t}]Hg\}^+ + RE^-$.

	***D*(Zn–ER)**	***D*(Hg–ER)**	***D*(Hg–ER) – *D*(Zn–ER)**
$[Tm^{Bu^t}]MSCH_2C(O)N(H)Ph$	103.67	102.85	−0.82
$[Tm^{Bu^t}]MSPh$	105.94	106.46	0.52
$[Tm^{Bu^t}]MSePh$	105.19	108.91	3.72

(a) cc-pVTZ(-f) (C, H, N, B, O, S) and LAV3P (Zn, Hg, Se, Te) basis sets.